Angular dependence of statistical distributions for backscattered signals: Modelling and application to multibeam echosounder data.

Gilles Le Chenadec*, Jean-Marc Boucher†, Xavier Lurton*, Jean-Marie Augustin*
*IFREMER
Service Acoustique et Sismique
BP 70, 29280 Plouzané, France
E-mail: gilles.le.chenadec@ifremer.fr
†École Nationale Supérieure de Télécommunications de Bretagne
BP 832, 29285 Brest Cedex, France
E-mail: JM.Boucher@enst-bretagne.fr

***Abstract*— A previous study ([1]) has shown that backscattered signal statistics, obtained from an acoustical imaging system, present a strong angular dependence. This paper deals with an extension of the proposed models to describe the intensity statistics fluctuations according to sonar resolution. Thus, the proposed model takes into account a wider variety of seabeds to provide an estimate of the order parameter of the K-law. Experimental data recorded by the EM1000 multibeam echosounder in shallow water provide the way to compare the different models on four different seafloors (mud, muddy sand, fine sand, coarse sand and a zone colonized by a bivalve population).**

I. Introduction

In high-resolution radar or sonar imaging, the K-distribution has shown interesting properties for describing the statistics of backscattered intensity. In addition to the fact that the distribution is in good agreement with empirical distributions, it advantageously provides a physical interpretation linked to the backscattering phenomenon ([2]). One of the particularities of acoustical seafloor imaging systems is that they map a wide zone across the ship's track. The instantaneous insonified area (or resolution cell) varies in a significant way, and causes the angular dependence of the distribution. With the aim of deriving information about backscattered intensity statistics, it appears essential to include these properties in order to differentiate acquisition parameters from scene parameters.

An angular study of the K-law properties is thus described in this paper, in order to determine the influence of the characteristics of acquisition systems.

Based on the model of distributed scatterers, Oliver ([3]) includes the correlation effects between scatterers and the finite size of the resolution cell and derives statistical moments of the backscattered intensity, distributed with a correlated K-law. Applied to either sonar or radar data, Oliver's model (OM) has shown good agreement with statistics. However, it did not include the angular evolution of statistics. Later, his model was applied by Hellequin to multibeam echosounder data ([1]) and supplemented to include the effect of the local bathymetry. The K-law was shown to adjust fairly well experimental data [1]). Although ADK model (called ADK model i.e Angular dependence of K-law) showed a capacity to model angular dependence of the K-law parameter, his approach is still limitative. First, a major drawback is the fact that the ADK model cannot include the diversity of seabed backscattered responses; its development is based on an over-simplified model of the backscattering strength. Secondly, the model has never been fitted to a whole set of different types of seabed.

The first part of this paper will present the Oliver's model and calculations leading to the statistics of backscattered intensity. The ADK model will be then explained in a second part. The third part will present an extension of ADK model (called EADK model) in order to consider seabed diversity and so to obtain a more realistic model. Finally, the three models (OM, ADK, EADK) are compared on experimental data recorded with a 100 kHz multibeam echosounder.

II. Oliver's model

Oliver's works are based on modelling backscattered intensity as a product ([4]):

$$I = R.S; \tag{1}$$

combining two different physical processes:

- The reflectivity underlying the scene R, depends on the average physical properties of the elementary scatterers.
- The *Speckle* phenomenon, assumedly not-correlated, is the consequence of the random distribution of these scatterers.

Thus, the response suggested to an acoustical imaging system will depend on these two physical processes. The model developed by Oliver proposes to incorporate in these processes two original assumptions. On the one hand, the correlation is planned to describe the surface model through the variable R. On the other hand, the wave scattering process takes into account the characteristics of the acquisition system.

A. Interface model

Oliver's choice to model the surface properties rises primarily from the work carried out by Jakeman ([5]) on the interaction of the electromagnetic waves with a rough surface. In this work ([6]), the model used is based on the theory of scattering elements:

- The surface is modelled by a dense network of scatterers described individually by their amplitudes a_j and their phases ϕ_j;
- The complex field $\mathcal{E}$ recorded for each image pixel is the incoherent sum of the contributions of N scatterers inside the resolution cell (or insonified area).

Thus,

$$\mathcal{E} = \sum_{j=1}^{N} a_j \exp\left(i\phi_j\right). \tag{2}$$

Whereas the traditional model of gaussian speckle corresponds to the limit case $N \rightarrow \infty$, Jakeman and Pusey ([7]) exploit the randomness of the effective number of scatterers N. They show that if N is controlled by a random process of birth, death and migration (N is distributed according to a negative binomial distribution), the recorded intensity is distributed according to a K law. This derivation suggests that the non-gaussian statistics[1] arise from a fluctuation of the effective number of scatterers inside the resolution cell.
Finally, starting from this model, Oliver ([8]) connects the order parameter of the Gamma distribution of R to the process of birth, death and migration.
Moreover, the Gamma law was proposed to describe the statistics of the hierarchical and fractal phenomena, well adapted to model natural surfaces ([9]).

The originality of the Oliver's model lies in the fact that it proves that the surface is not entirely described by the first-order statistics (probability density) since its understanding implies the study of its correlation properties ([4]).
Thus, the surface is described by the assumedly stationary random variable R, distributed according to the Gamma law $f_R(R)$ and by spatial correlation coefficient ρ_r, whose characteristics are given by:

$$\begin{cases} f_R(R) = & \left(\frac{\nu}{\mathbb{E}[R]}\right)^{\nu} \frac{R^{\nu-1}}{\Gamma(\nu)} \exp\left(-\frac{\nu R}{\mathbb{E}[R]}\right), \\ \mathbb{E}[R^m] = & \left(\frac{\mathbb{E}[R]}{\nu}\right)^{m} \frac{\Gamma(\nu+m)}{\Gamma(\nu)}, \\ \rho_R(\xi) = & \frac{\mathbb{E}[R(\xi_1)R(\xi_2) - \mathbb{E}[R]^2]}{\mathbb{E}[R^2] - \mathbb{E}[R]^2}. \end{cases} \quad (3)$$

where $\xi = |\xi_1 - \xi_2|$ is the distance between samples positioned in ξ_1 and ξ_2.

Model of spatial correlation spectrum: The spectra considered in this paper is 2D-gaussian:

$$\rho_R(x, y) = \exp\left(-\frac{x^2}{Lc_x^2}\right).\exp\left(-\frac{y^2}{Lc_y^2}\right). \quad (4)$$

where $x = x_1 - x_2$, $y = y_1 - y_2$ et (Lc_x, Lc_y) are the spatial correlation lengths in two dimensions.

B. The scattering process

Let us assume that we image a homogeneous region whose randomness is described by a correlated Gamma law (see II-A). The backscattered intensity $I(\xi)$ at position ξ arising from a scene with complex scattering amplitude[2] $A(\xi)$ at position ξ is given by ([3]):

$$I(\xi) \equiv |\mathcal{E}(\xi)|^2 = \int_{\mathbb{R}^2} \Big[A(\xi_1)A^*(\xi_2)h(\xi-\xi_1)h^*(\xi-\xi_2)\Big] d\xi_1 d\xi_2, \quad (5)$$

where h is the spatial impulse response of the sonar (trace of the signal on the bottom), * indicate the complex conjugation and $\mathcal{E}$ is the complex backscattered field .
In the case of a multibeam echosounder, the function h is approached by the function:

$$h(x) = \begin{cases} \frac{1}{La_x} & \text{if } -\frac{La_x}{2} \leq x \leq \frac{La_x}{2}; \\ 0 & \text{otherwise.} \end{cases} \quad (6)$$

[1]Statistics whose complex field does not satisfy any more the fully developed speckle model or traditional Gaussian one.
[2]linked by $R = |A(\xi)|^2$.

where La_x is the length of the resolution cell. In the 2D case, the function $h(x, y)$ is a separable function in x and in y; $h(x, y) = h(x).h(y)$.
Upon taking the ensemble average over all speckle realizations, one observes that the contributions from various positions of the backscattered field A average out because of the random phases of scattering elements. This leads to the interesting property:

$$\mathbb{E}[I(\xi)] = \int_{\mathbb{R}} \Big[\mathbb{E}[|A(\xi)|^2]|h(\xi-\xi_1)|^2\Big] d\xi_1 = \mathbb{E}[R(\xi)]. \quad (7)$$

C. Derivation of the statistical moments of the scattered intensity

Oliver defines the means of deriving the normalized moments of the measured intensity by taking account at the same time the correlation of the scatterers and specificities of the imaging system:

$$\frac{\mathbb{E}[I^n]}{\mathbb{E}[I]^n} = \frac{\Gamma(L+n)}{L^n\Gamma(L)} \cdot \int_{\mathbb{R}^n} \left[\frac{\mathbb{E}[R(\xi_1)\dots R(\xi_n)]}{\mathbb{E}[R]^n} |h(\xi_1)|^2 \dots |h(\xi_n)|^2\right] d\xi_1 \dots d\xi_n; \quad (8)$$

where $\xi_i = (x_i, y_i)$ is the position of the i-th scatterer.
Moreover, R is supposed to be stationary and characterized by the autocorrelation function (Eq. (3)):

$$\mathbb{E}[R(\xi_1)R(\xi_2)] = \mathbb{E}[R]^2 \left(1 + \frac{\rho_R(\xi_1 - \xi_2)}{\nu}\right). \quad (9)$$

Thus, taking $n = 2$, using (9) and replacing by the expression of h, the second order normalized moment becomes:

$$\frac{\mathbb{E}[I^2]}{\mathbb{E}[I]^2} = \frac{L+1}{L} \frac{1}{La_x^2.La_y^2} \int_{-\frac{La_x}{2}}^{\frac{La_x}{2}} \int_{-\frac{La_y}{2}}^{\frac{La_y}{2}} \left[\frac{\mathbb{E}[R(\xi_1)R(\xi_2)]}{\mathbb{E}[R]^2}\right] d\xi_1 d\xi_2; \quad (10)$$

$$= \frac{L+1}{L} \frac{1}{La_x^2.La_y^2} \int_{-\frac{La_x}{2}}^{\frac{La_x}{2}} \int_{-\frac{La_y}{2}}^{\frac{La_y}{2}} \left[1 + \frac{\rho_R(\xi_1 - \xi_2)}{\nu}\right] d\xi_1 d\xi_2. \quad (11)$$

For a roughness characterized by (4), the calculation of (10) becomes:

$$\frac{\mathbb{E}[I^2]}{\mathbb{E}[I]^2} = \frac{L+1}{L} \left[1 + \frac{F_{Gauss}(\gamma_x)F_{Gauss}(\gamma_y)}{\nu}\right]; \quad (12)$$

where

$$\begin{cases} F_{Gauss}(x) = \frac{\sqrt{\pi}}{x}.\mathrm{erf}(x) + \frac{\exp(-x^2)}{x^2} - x^{-2}, \\ \gamma_x = \frac{La_x}{Lc_x}, \\ \gamma_y = \frac{La_y}{Lc_y}, \end{cases} \quad (13)$$

and erf is the error function.

Determination of ν_K as from the normalized moment of 2nd order: From an analytical point of view, the normalized moment of 2nd order associated with a K-law, is derivable:

$$\frac{\mathbb{E}[I^2]}{\mathbb{E}[I]^2} = \left(\frac{L+1}{L}\right)\left(1 + \frac{1}{\nu_K}\right). \quad (14)$$

The order parameter of the K-law can be obtained thanks to the order parameter of the Gamma law and to the sounder specificities:

$$\nu_K = \frac{\nu}{F_{Gauss}(\gamma_x)F_{Gauss}(\gamma_y)}. \quad (15)$$

III. ADK MODEL

A. Presentation

In his PhD ([10]), Hellequin resumes Oliver's work in order to completely separate the acquisition system properties from the seabed properties. Confronting the results of Oliver with experimental data, he proposes an extension of Oliver's model ([10]). The main assumption is that the order parameter ν of the law of R (correlated Gamma law) depends on the angle of incidence.

Indeed, multibeam echosounder data do not allow an exact estimate of the incident angles θ_{inc}. The bathymetric capacity has not the same acrosstrack resolution as the imagery one. Consequently, bathymetry is interpolated for the missing probes ([10]). The angle of incidence of the signal is then calculated by the relation $\theta_{inc} = \theta_{emi} - \phi_{bat}$, where θ_{emi} is emission angle and ϕ_{bat} is the bottom slope angle. The lack of bathymetric data thus randomizes local slopes ϕ_{bat} and consequently incident angles θ_{inc}.

The model assumes a Gaussian distribution of the slopes with a zero mean and a standard deviation σ:

$$f_{\phi_{bat}}(\phi) = \frac{1}{\sqrt{2\pi}\sigma} \exp(-\frac{\phi^2}{2\sigma^2}) \tag{16}$$

$$\Longrightarrow f_{\theta_{inc}}(\phi) = \frac{1}{\sqrt{2\pi}\sigma} \exp(-\frac{(\theta_{emi}-\phi)^2}{2\sigma^2}). \tag{17}$$

The distribution associated with the new random variable θ_{inc} is thus gaussian ($\mathcal{N}(\theta_{emi}, \sigma^2)$).

In addition, taking into account the product model (1), together with (7):

$$\mathbb{E}[I] = \mathbb{E}[R] = \mathbb{E}[BS(\theta_{inc})], \tag{18}$$

The backscattering angular model used in ([10]) is a simplified model combining:

- a Gaussian law for the specular angles,
- a Lambert law for the grazing angles:

$$BS(\theta_{inc}) = A\exp(-\alpha\theta_{inc}^2) + B\cos^2(\theta_{inc}), \tag{19}$$

It is then possible to calculate the m-order moments of R based on (18):

$$\mathbb{E}[R]^m \quad = \quad \int_{\mathbb{R}} BS^m(\theta_{inc}) f_{\theta_{inc}}(\theta_{inc}) d\theta. \tag{20}$$

The first two moments are obtained as:

$$\mathbb{E}[R] = C_1.\exp\left(-D_1\theta_{emi}^2\right) + \frac{B}{2}.\left[1+\cos\left(2\theta_{emi}\right)\exp\left(-2\sigma^2\right)\right]; \tag{21}$$

$$\mathbb{E}[R^2] = I_1 + I_2 + I_3; \tag{22}$$

where

$$\begin{cases} I_1 = C_2.\exp\left(-D_2\theta_{emi}^2\right); \\ I_2 = B.C_1.\exp\left(-D_1\theta_{emi}^2\right)\left(1+\exp(-2C_3)\cos(\frac{2\theta_{emi}}{1+2\alpha\sigma^2})\right); \\ I_3 = \frac{B^2}{8}\left(3+4\cos(2\theta_{emi})\exp(-2\sigma^2)+\cos(4\theta_{emi})\exp(-8\sigma^2)\right); \end{cases} \tag{23}$$

and

$$\begin{cases} C_1 = \frac{A}{\sqrt{1+2\alpha\sigma^2}}, \quad D_1 = \frac{\alpha}{1+2\alpha\sigma^2}, \\ C_2 = \frac{A^2}{\sqrt{1+4\alpha\sigma^2}}, \quad D_2 = \frac{2\alpha}{1+4\alpha\sigma^2}, \\ C_3 = \frac{\sigma^2}{1+2\alpha\sigma^2}. \end{cases} \tag{24}$$

Then, the variable R, assumedly distributed according to a Gamma law, provides the property:

$$\frac{\text{var}(R)}{\mathbb{E}[R]^2} = \frac{1}{\nu}. \tag{25}$$

Lastly, (15) makes it possible to obtain the order parameter of the K-law by integrating the Oliver's model.

B. Extension to a more realistic backscattering model

The choice to model BS in ([10]) is too simple to take into account the whole set of angular behaviors of the seabed. A model in law of β-Lambert for the grazing angles (replacement of $\cos^2(\theta_{inc})$ by $\cos^\beta(\theta_{inc})$ in (19)) would be better justified in comparison with measurements of BS (see IV).

Unfortunately, the analytical calculation of the moments of the underlying reflectivity R (20) is then not possible (because of the exponent β of the cosine function). The variable ϕ_{bat} describing the bathymetry slopes being centered on 0, a limited development of the function $cos^\beta(\theta_{emi} - \phi)$ is however possible and thus gives rise to a new more complete model (called thereafter **EADK** model i.e Extended model of angular dependence of the K-law).

Thus, by carrying out a development limited in ϕ_{bat} around 0 to order 3, (19) becomes:

$$BS(\theta_{inc}) = A\exp(-\alpha\theta_{inc}^2) + B\cos^\beta(\theta_{inc}), \tag{26}$$

$$= A.\exp(-\alpha(\theta_{emi}-\phi)^2) + (b_1 + b_2\phi + b_3\phi^2 + b_4\phi^3). \tag{27}$$

where:

$$\begin{cases} b_1 = B.\cos^\beta(\theta_{emi}), \\ b_2 = B.\beta.\cos^{\beta-1}(\theta_{emi}).\sin(\theta_{emi}), \\ b_3 = \frac{b_1.\beta}{2}\left[(\beta-1).\tan^2(\theta_{emi})-1\right] \\ b_4 = \frac{b_2.\beta}{6}\left[(\beta^2-3\beta+2)(1+\tan^2(\theta_{emi}))-\beta^2\right]. \end{cases} \tag{28}$$

By taking again the notations of (24), the first two-moments become:

$$\mathbb{E}[R] = C_1.\exp\left(-D_1\theta_{emi}^2\right) + b_1 + b_3.\sigma^2; \tag{29}$$

$$\mathbb{E}[R^2] = J_1 + J_2 + J_3; \tag{30}$$

where

$$\begin{cases} J_1 = C_2.\exp\left(-D_2\theta_{emi}^2\right), \\ J_2 = b_1^2 + (b_2^2+2b_1b_3)\sigma^2 + 3(b_3^2+2b_2b_4)\sigma^4 + 15b_4^2\sigma^6, \\ J_3 = 2C_1.\exp\left(-D_1\theta_{emi}^2\right)(b_1 + b_3C_3 + 6b_4C_3^2 \\ \qquad + 2\alpha b_2C_3\theta_{emi} + 4\alpha^2C_3^2b_3\theta_{emi}^2 + 8\alpha^3C_3^3b_4\theta_{emi}^3). \end{cases} \tag{31}$$

IV. EXPERIMENTAL CONFRONTATION

A. Presentation of the data

The experimental data come from 5 sedimentary zones from the Bay of Douarnenez (France) mapped with a Simrad EM1000 multibeam echosounder:

- 2 zones (1 et 6) colonized by a bivalve population;

- 1 coarse sand zone (zone 4);
- 1 fine sand zone (zone 5);
- 1 muddy sand zone (zone 2).

After correction of the data (according to the procedure described in [1]), an acoustic image of the seabed backscattering is plotted with a resolution of 1 meter. The intensity data is collected for the homogeneous zones described above. Next, they are sorted into angular sectors of 5 degrees from -75 degrees (port side) up to 75 degrees (starboard). The empirical densities are then calculated.

The estimate of the K-law parameters is based on the A-statistics ([11]). The K-law is then put in competition with a set of common laws representing the statistics of natural surfaces imagery (negative Exponential, Weibull, Log-normal...); the criterion of fitting being the Kolmogorov-Smirnov test.

Thus, after checking the good adequacy of the K-law on the whole set of angular sectors, the two parameters of the K-law (the average expressed in dB and the order parameter ν_K) for the 5 sedimentary zones are represented in figures (1), (2) and (3). However, the following analysis will relate exclusively to the K-law order parameter.

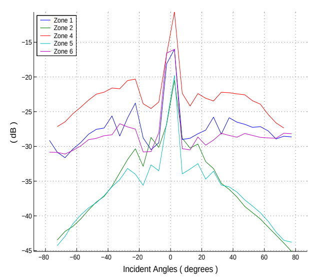

Fig. 1. Angular dependence of the mean backscatter intensity (in dB) for the 5 sedimentary zones.

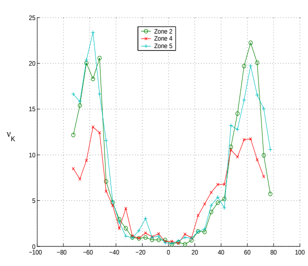

Fig. 2. Angular dependence of the order parameter for 3 sedimentary zones.

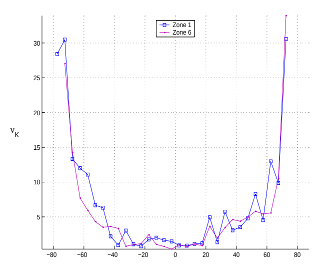

Fig. 3. Angular dependence of the order parameter for 2 sedimentary zones.

Before any further analysis, it is reminded that the K-law provides a large set of different shapes; from the Rayleigh law to the negative Exponential law. The K-law becomes an Exponential one (for intensity data) when its order parameter $\nu_K \longrightarrow \infty$. From previous studies (e.g. [1], [4]), the interpretation of the values of ν_K according to seabed dependence can be carried out like this:

- Low values of ν_K correspond to heterogeneous interface. This can be explained in various way. A high-resolution imaging system has a confined size of resolution cell and thus will be able to follow accurately the details of seafloor relief ([1]). In statistical terms, the number of scatterers inside the resolution cell is small and the complex statistics will not be gaussian any more (see II-A). On another hand, the bottom may be perfectly homogeneous but have a significant roughness. In this case, whatever the size of the resolution cell is, only a small number of scatterers return a dominating echo. Then, the statistics will be in the same way not gaussian.
- On the opposite side, large values of ν_K correspond to homogeneous interface; a significant size of the resolution cell average out all the contributions of the scatterers and/or the roughness of surface is smooth.

The angular dependence of the order parameter is split into three modes (Fig. (2) and (3)):

- For angles close to the vertical (typically $|\theta| < 20^0$):
  The order parameter, with very small values, does not allow to discriminate between seabed types. Its low values indicate a strong heterogeneity. This type of heterogeneity is primarily related to the acoustic response of the seabed and sounder inside this angular sector. Indeed, in this zone, the signal fluctuations, especially strong, are due to the extended insonified area, and to the quick angular variations of the backscattering strength.
- For intermediate angles between specular and grazing:
  The curves of the very rough zones (zones 1 and 6 (Bivalves), Fig. (3)) have a softer slope than the smoother zones (Fig. (2)).
- For grazing angles, a characteristic inversion of slope is observable on Fig. (2) contrarily to curves of Fig. (3) which keep their characters of monotonous slopes.

The global increase in the order parameter ν_K while moving away from the specular zone can be explained by the angular evolution of the insonified surface. When one moves away from the specular zone to go until the grazing angles, the insonified area[3] increases. The resolution cell thus includes a greater effective number N of scatterers; in other words, the central limit theorem applies and the K-law is a negative exponential law (the statistics follow the gaussian complex model or the Rayleigh law in amplitude). The Oliver's model incorporates this concept of size of the resolution cell showing its interest.

For the second mode, the slope of the order parameter is softer for the rough seafloor. Indeed, roughness quantifies, within the resolution cell of resolution, the number of scatterers contributing individually to the total answer. Thus, the rougher the bottom is, the smaller the number of scatterers dominates the response. Then, the order parameter will present lower values; the seafloor will be considered heterogeneous in terms of roughness.

An cut-off angle separating the last two modes is definitely visible on the Fig. (2); it looks characteristic of the seabed. Rough seafloors do not seem to present such an cut-off angle; one can however assume that this angle is present but is invisible for the available angles.

On another side, the differences in evolution according to the seafloor for the more grazing angles is intriguing. Indeed, the types of bottom, showing this characteristic, are, on the one hand not very rough and on the other hand homogeneous in sedimentary terms. The answer is provided at the same time by the analysis of curves of $BS(\theta)$ (Fig. 1) and by the process of information extraction. Indeed, the main reason is the lack of bathymetric resolution ([1]) and thus uncertainty on the incident angles of the backscattered intensity. Consequently, the slope of $BS(\theta)$ takes a considerable importance in the estimate of the moments (and thus the order parameter). Zones 2, 4 and 5 show $BS(\theta)$ with a significant slope for the grazing angles contrarily to zones 1 and 6 showing $BS(\theta)$ almost flat, characteristic of very rough seabeds.

[3] or the size of the resolution cell.

B. Results on a homogeneous zone

In this section, experimental results are fitted on the three different models:

- the Oliver's model (OM),
- the Hellequin's model of angular dependence (ADK),
- the extension of ADK model (EADK).

Initially, the study will be carried out on an "homogeneous" fine sand zone which includes the following features:

- sedimentary homogeneity,
- smooth bathymetry,
- order parameter decreasing at grazing angles,
- good accordance of $BS(\theta)$ with the model in cos^2.

The first stage leading to the determination of the parameters of ADK and EADK model consists in fitting the measured $BS(\theta)$. Fig. 4 shows the result.

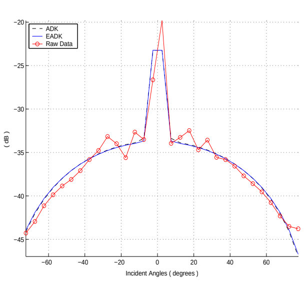

Fig. 4. $BS(\theta)$ for an homogeneous fine sand zone and its ADK and EADK fits.

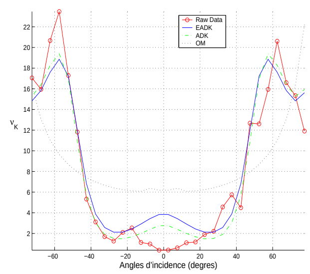

Fig. 5. Order parameter ν_K of the K-law for an homogeneous fine sand zone and the ADK and EADK fits.

Adjustments are satisfactory within the meaning of the average quadratic error (Tab. I and II). EADK model leads numerically to $\beta = 1.935$; close to the theoretical value of 2 for which the zone was selected. The curves of the ADK and EADK models are superimposed.

A light port-starboard asymmetry of the measurement curve is observed, certainly coming from an inaccurate bathymetric correction. The fittings on the order parameter of the K-law, obtained on the one hand for the Oliver's model (parameters Lc_x and Lc_y: spatial correlation lengths of the image and ν order parameter of the assumedly angularly independent Gamma law) and on the other by ADK and EADK models (parameters Lc_x, Lc_y, σ standard deviation of the incident angles and the BS parameters) are represented in Fig. 5. Asymmetry is observed again on the raw data. Taking into account the natural variability, it is indeed difficult to find sedimentary homogeneous zones over a 250 meter range. The developed model undoubtedly must be applied distinctly to port side then to starboard. However, Fig. 5 clearly shows that Oliver's model is unable to provide the appropriate angular evolution of the order parameter of the K-law; ADK and EADK models show a better adequacy with data for grazing angles. However, for specular angles, the fittings move away from the real data. The model validity is thus to be discussed for this angular sector.

Quantitatively, the average standard deviation (rms) between the Oliver's model and the real data is 5.751. This variation for the ADK model (respectively EADK) is 1.95 (resp. 2.21).

In conclusion, for an homogeneous zone, the ADK and EADK models fit the experimental data better than the Oliver's one. Indeed, the latter does not make it possible to take into account the singularities of some seabed types. In addition, these first results highlight the fact that the angular evolution is not symmetrical. Indeed, in spite of the precautions taken to consider an homogeneous zone, small events (due to a light slope or a estimation noise) disturb the order parameter estimation ν_K and create an angular dissymmetry. Consequently, the next fittings will be carried out distinctly with port side then with starboard.

C. Results on the whole set of seabed

A quantitative analysis was carried out on the whole set of the zones. Thus, Fig. (6), (9), (12), (15) and (18) show the fittings on measured BS for the two models (ADK and EADK). In order to quantify the differences, the average standard deviations (rms) are computed for each fitting and are retranscribed in the Tab. (I) and (II) with the models parameters.

	ADK model				
Facies	**rms**	A (dB)	α	B (dB)	β
Zone 1	**3.46**	-15.2	328	-23.8	2
Zone 2	**2.18**	-21.6	309	-33.1	2
Zone 4	**2.14**	-11.1	459	-20.1	2
Zone 5	**1.28**	-21.1	310	-33.6	2
Zone 6	**3.73**	-11.9	601	-25.0	2

TABLE I
FITTINGS ON BS FOR THE ADK MODEL.

	EADK model				
Facies	**rms**	A (dB)	α	B (dB)	β
Zone 1	**1.52**	-13.4	487	-27.3	0.35
Zone 2	**2.04**	-21.2	389	-32.2	2.43
Zone 4	**1.39**	-11.1	405	-21.9	0.93
Zone 5	**1.27**	-20.5	370	-33.7	1.95
Zone 6	**1.12**	-13.0	433	-22.8	0.12

TABLE II
FITTINGS ON BS FOR THE EADK MODEL.

EADK model obviously shows better quality of fitting; this model takes into account a larger variety of seabed types. Only the fitting of zone 2 is questionable (Fig. 9); EADK model is then not better than the ADK one. The constant slope of BS for this bottom type could be modelled more precisely by the addition of a transitory component (Gaussian-shaped) linking between the specular sector and the grazing angles sector ([12]).

The remaining figures represent for each sedimentary zone, fittings of the order parameter ν_K on the side port side (Fig. (7), (10), (13), (16) and (19) and on the starboard (Fig. (8), (11), (14), (17) and (20), of the three models (Oliver, ADK and EADK).

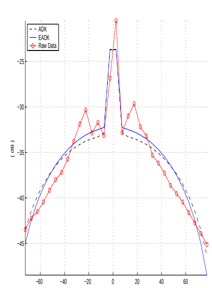

Fig. 9. Fitting of BS; zone 2 (muddy sand).

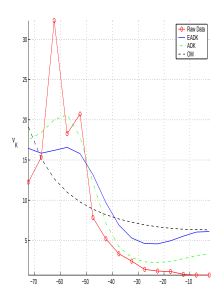

Fig. 10. Fitting of ν_K; zone 2 (port side).

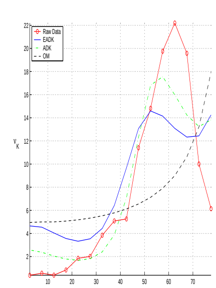

Fig. 11. Fitting of ν_K; zone 2 (starboard).

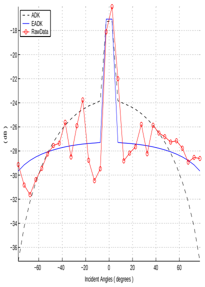

Fig. 6. Fitting of BS; zone 1 (bivalve).

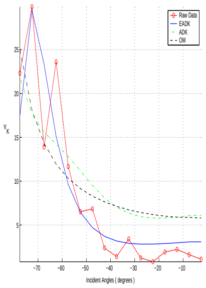

Fig. 7. Fitting of ν_K; zone 1 (port side).

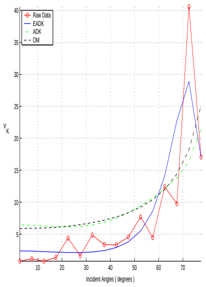

Fig. 8. Fitting of ν_K; zone 1 (starboard).

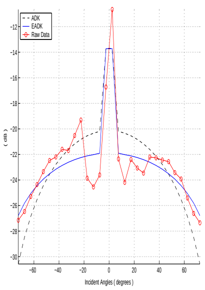

Fig. 12. Fitting of BS; zone 4 (coarse sand).

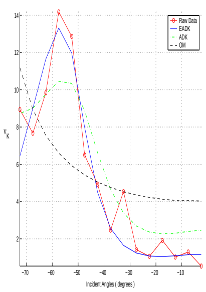

Fig. 13. Fitting of ν_K; zone 4 (port side).

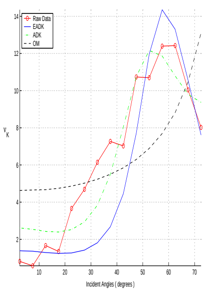

Fig. 14. Fitting of ν_K; zone 4 (starboard).

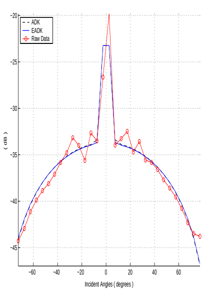

Fig. 15. Fitting of BS; zone 5 (fine sand).

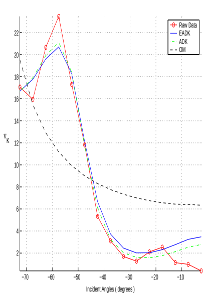

Fig. 16. Fitting of ν_K; zone 5 (port side).

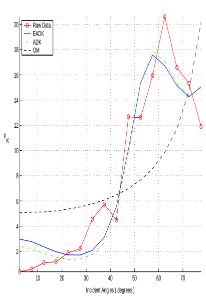

Fig. 17. Fitting of ν_K; zone 5 (starboard).

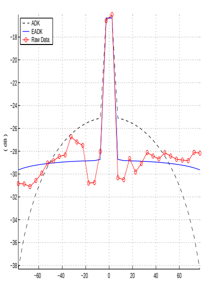

Fig. 18. Fitting of BS; zone 6 (bivalve).

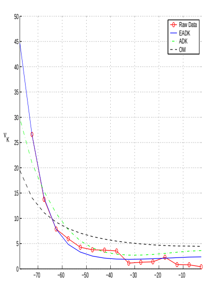

Fig. 19. Fitting of ν_K; zone 6 (port side).

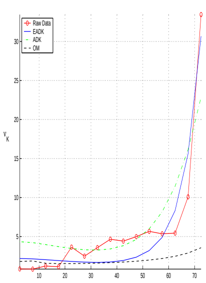

Fig. 20. Fitting of ν_K; zone 6 (starboard).

Once again, the standard deviations between experimental and model measurements were calculated and are retranscribed in Tab. III and IV together with the fitted parameters of the models.

Facies	Oliver's model			
	rms	Lc_x	Lc_y	ν
Zone 1 port side	**5.53**	4.50	0.190	1.14
Zone 1 starboard	**7.05**	4.98	0.350	1.84
Zone 2 port side	**7.50**	4.99	0.304	2.87
Zone 2 starboard	**6.77**	4.99	0.710	2.89
Zone 4 port side	**3.42**	4.99	0.672	2.04
Zone 4 starboard	**3.20**	4.99	0.600	2.16
Zone 5 port side	**5.80**	4.99	0.250	1.61
Zone 5 starboard	**5.16**	4.95	0.210	2.10
Zone 6 port side	**4.34**	4.99	0.160	0.71
Zone 6 starboard	**5.84**	4.99	0.120	0.59

TABLE III

RESULTS FOR FITTING ON ν_K FOR OLIVER'S MODEL.

Facies	ADK model			
	Rms	Lc_x	Lc_y	σ
Zone 1 port side	**5.39**	4.99	0.130	19.91
Zone 1 starboard	**7.43**	4.99	0.126	21.74
Zone 2 port side	**4.05**	5.00	0.163	14.46
Zone 2 starboard	**3.21**	5.00	0.225	13.78
Zone 4 port side	**1.76**	4.99	0.360	15.68
Zone 4 starboard	**1.40**	5.00	0.347	15.18
Zone 5 port side	**1.21**	4.99	0.170	13.66
Zone 5 starboard	**2.10**	5.00	0.203	13.75
Zone 6 port side	**2.31**	4.99	0.080	19.07
Zone 6 starboard	**3.95**	4.99	0.070	19.57

TABLE IV

RESULTS FOR FITTING ON ν_K FOR ADK MODEL.

Facies	EADK model			
	Rms	Lc_x	Lc_y	σ
Zone 1 port side	**3.64**	4.97	0.089	23.03
Zone 1 starboard	**4.85**	4.87	0.110	22.14
Zone 2 port side	**5.73**	5.01	0.127	15.00
Zone 2 starboard	**4.48**	5.02	0.170	13.70
Zone 4 port side	**1.28**	4.99	0.780	15.55
Zone 4 starboard	**2.30**	3.71	0.600	16.14
Zone 5 port side	**1.50**	4.98	0.145	13.83
Zone 5 starboard	**2.13**	5.00	0.170	13.88
Zone 6 port side	**1.10**	5.00	0.090	23.84
Zone 6 starboard	**2.40**	5.00	0.106	22.99

TABLE V

RESULTS FOR FITTING ON ν_K FOR EADK MODEL.

Firstly, the fittings based on the simple Oliver's model are poor, showing once again the limitation of this model to follow the angular dependence of the order factor of the K-law. The improvement brought by ADK and EADK models on the model of Oliver is undeniable on the whole data set.
In order to compare the ADK and EADK models, three points can be distinguished:

- The angular behavior of BS for zone 5 leads to a law in $\beta = 2$. The fittings for the two models are hence quasi-identical (Fig. 16 and 17). Thus, the limited development carried out for the calculation of EADK model does not seem to have generated notable skew. Moreover, having carried out distinct fittings for port side and starboard makes it possible to gain in precision compared to the results of the previous section (realized on the same zone).

- The fittings on zones 1, 4 and 6 are definitely better (table IV) with the EADK model. For this type of zone characterized by strong roughness (bivalve population (zones 1 and 6) and coarse sand (zone 4)), the angular behavior of BS moves away largely from the $\cos^2$ law (zone 1: $\beta = 0.35$, zone 4: $\beta = 0.93$ and zone 6: $\beta = 0.12$). The importance of the BS model is thus proved and this development of the new model justified.
- For zone 2, the fittings are poor; the models do not retranscribe in a reasonable way the angular behavior of the order parameter (Fig. 10 and 11). The modelling of BS for this zone was not found sufficient. An extension of the model of BS could then be considered.

Finally, even if the fittings on the grazing angles seem correct, those on the specular angles show problems. Indeed, models don't fit the specular zone. This variation with angle is similar to the one carried out for physical modelings of backscattering strength ([13]):

- At specular angles, models are based on the existence of tangent planes.
- At grazing angles, the laws of the geometrical diffusion apply and the model of the small perturbations is used.

If the small-perturbation model is used at grazing angles, surface roughness dominates the process and so interference phenomena appears within the resolution cell. Then, the model of the distributed scatterers is valid. For specular angles, the existence of tangent planes assume that a small number of scatterers dominates the process; invalidating hypothesis of theory of the scattering elements. Then, this could explain why the fitting of the order parameter is not as good in this angular sector.

V. Conclusion

In this paper, a model is proposed in order to describe the angular dependence of K-law order parameter. This model is based on the process of image formation; it takes into account both acquisition system and seafloor. A study on real shallow water data recorded by a multibeam echosounder has been realized. The empirical K-law order parameter computed show a characteristic evolution with a cut-off angle. The new model has showed a good capacity to describe the angular evolution of ν_K compare to others models; Oliver's one is not able to fit the cutting angle evolution and the ADK one is less precise. The limitation of this new model is the specular zone where the statistic model is not valid.

References

[1] L. Hellequin, J-M.Boucher, and X.Lurton, "Processing of high frequency multibeam echosounder data for seafloor characterization," *IEEE Trans. Journal of Oceanic Engineering*, vol. 28, no. 1, 2003.

[2] E. Jakeman, "Non gaussian models for the statistics of scattered waves," *Advances in Physics*, vol. 37, no. 5, pp. 471–529, 1988.

[3] C. Oliver, "A model for non-rayleigh scattering statistics," *Optica Acta*, vol. 31, no. 6, pp. 701–722, 1984.

[4] C. Oliver and S. Quegan, *Synthetic Aperture Radar Images*. Artech House, 1998.

[5] E. Jakeman *et al.*, "Significance of k distributions in scattering elements," *Physical Review Letters*, vol. 40, no. 9, pp. 546–550, 1978.

[6] C. Oliver, "The interpretation and simulation of clutter textures in coherent images," *Inverse Problems*, vol. 2, pp. 481–518, 1986.

[7] E. Jakeman and P. Pusey, "A model for non-rayleigh sea echo," *IEEE Trans.AntennasPropagation*, vol. 24, pp. 806–814, 1976.

[8] C. Oliver and R. Tough, "On the simulation of correlated k-distributed random clutter," *Opt.Acta*, vol. 33, pp. 223–250, 1986.

[9] Mandelbrot, *Fractals*. Freeman, 1977.

[10] L. Hellequin, "Analyse statistique et spectrale des signaux de sondeurs multifaisceaux em950: Application à l'identification des fonds sous marins," Ph.D. dissertation, Université de Rennes1 U.F.R. Structures et Propriétés de la Matière, December 1998.

[11] P. Lombardo and C. Oliver, "Estimation of texture parameters in k-distributed clutter," *IEE Proc., Radar Sonar Navig.*, vol. 141, no. 4, pp. 196–204, 1994.

[12] X. Lurton, *An Introduction to Underwater Acoustics: Principles and Applications*. Springer-Verlag, 2002.

[13] H. Medwin and C. Clay, *Fundamentals of Acoustical Oceanography*. Academic Press, 1998.